NeuroImage xxx (2014) xxx–xxx

Contents lists available at ScienceDirect

NeuroImage

journal homepage: www.elsevier.com/locate/ynimg

Behavioral, metabolic and functional brain changes in a rat model of chronic neuropathic pain: A longitudinal MRI study

Catherine S. Hubbard [a], Shariq A. Khan [a], Su Xu [e,f], Myeounghoon Cha [b], Radi Masri [b,c,d], David A. Seminowicz [a,c,*]

[a] Department of Neural and Pain Sciences, University of Maryland School of Dentistry, USA
[b] Department of Endodontics, Prosthodontics and Operative Dentistry, University of Maryland School of Dentistry, USA
[c] Program in Neuroscience, University of Maryland School of Medicine, Baltimore, MD 21201, USA
[d] Department of Anatomy and Neurobiology, University of Maryland School of Medicine, Baltimore, MD 21201, USA
[e] Department of Diagnostic Radiology and Nuclear Medicine, University of Maryland School of Medicine, Baltimore, MD 21201, USA
[f] Core for Translational Research in Imaging @ Maryland, University of Maryland School of Medicine, Baltimore, MD 21201, USA

ARTICLE INFO

Article history:
Accepted 9 December 2014
Available online xxxx

ABSTRACT

Peripheral neuropathy often manifests clinically with symptoms of mechanical and cold allodynia. However, the neuroplastic changes associated with peripheral neuropathic pain and the onset and progression of allodynic symptoms remain unclear. Here, we used a chronic neuropathic pain model (spared nerve injury; SNI) to examine functional and metabolic brain changes associated with the development and maintenance of mechanical and cold hypersensitivity, the latter which we assessed both behaviorally and during a novel acetone application paradigm using functional MRI (fMRI). Female Sprague–Dawley rats underwent SNI (n = 7) or sham (n = 5) surgery to the left hindpaw. Rats were anesthetized and scanned using a 7 T MRI scanner 1 week prior to (pre-injury) and 4 (early/subchronic) and 20 weeks (late/chronic) post-injury. Functional scans were acquired during acetone application to the left hindpaw. ^{1}H magnetic resonance spectroscopy was also performed to assess SNI-induced metabolic changes in the anterior cingulate cortex (ACC) pre- and 4 weeks post-injury. Mechanical and cold sensitivity, as well as anxiety-like behaviors, were assessed 2 weeks pre-injury, and 2, 5, 9, 14, and 19 weeks post-injury. Stimulus-evoked brain responses (acetone application to the left hindpaw) were analyzed across the pre- and post-injury time points. In response to acetone application during fMRI, SNI rats showed widespread and functionally diverse changes within pain-related brain regions including somatosensory and cingulate cortices and subcortically within the thalamus and the periaqueductal gray. These functional brain changes temporally coincided with early and sustained increases in both mechanical and cold sensitivity. SNI rats also showed increased glutamate within the ACC that correlated with behavioral measures of cold hypersensitivity. Together, our findings suggest that extensive functional reorganization within pain-related brain regions may underlie the development and chronification of allodynic-like behaviors.

Introduction

Peripheral neuropathic pain is a chronic, debilitating condition resulting from disease or direct nerve injury. Clinical features include pain evoked by low threshold tactile and cool temperature stimuli that normally do not elicit pain, termed mechanical and cold allodynia, respectively (Sandkuhler, 2009). A partial denervation rodent model known as spared nerve injury (SNI) leads to early and sustained mechanical and cold hypersensitivity, which closely resemble the clinical features of mechanical and cold allodynia in patients with peripheral neuropathies (Decosterd and Woolf, 2000). Thus, SNI represents a tractable animal model for investigating the underlying brain mechanisms associated with the development and maintenance of chronic neuropathic pain and allodynic-like behaviors, and is particularly well-suited for longitudinal investigations employing structural and functional MRI (fMRI).

Typically, studies investigating brain changes associated with neuropathic pain models in rodents have examined early time points, within days to less than a month following injury (Chang et al., 2014; Mutso et al., 2012). However, volumetric reductions in the rat prefrontal cortex (PFC) manifest as late as four months following SNI, and coincide with the appearance of anxiety-like behaviors (Seminowicz et al., 2009). Furthermore, volumetric reductions in other cortical regions, including the anterior cingulate cortex (ACC), primary somatosensory cortex (S1), and insula were correlated with mechanical hypersensitivity in SNI rats, indicating that peripheral nerve injury induced long-term structural changes in pain-related brain regions that were accompanied

* Corresponding author at: Department of Neural and Pain Sciences, University of Maryland School of Dentistry, 650 West Baltimore Street, 8 South, Baltimore, MD 21201, USA. Fax: +1 410 706 0865.
E-mail address: dseminowicz@umaryland.edu (D.A. Seminowicz).

http://dx.doi.org/10.1016/j.neuroimage.2014.12.024
1053-8119/

by behavioral signs of mechanical allodynia. Neuroimaging studies using experimental models of mechanical and cold allodynia in patients with various chronic neuropathic pain conditions have shown functional reorganization in similar brain areas including the ACC, somatosensory cortices, thalamus, and insula (Becerra et al., 2006; Maihofner et al., 2006; Peyron et al., 2004; Witting et al., 2006). Together, these findings suggest that the brain undergoes widespread structural and functional changes following peripheral nerve damage which, over extended periods of time, may lead to the transition of pain from an acute and adaptive state to a chronic, maladaptive disease state. The mechanisms and time course of these events, and extent of the cortical and subcortical areas involved in this transition are not well-understood.

The primary aim of the current study was to identify early (subchronic) and late (chronic) functional brain changes associated with the development and maintenance of cold hypersensitivity using a neuropathic pain model of cold allodynia in SNI rats during a novel stimulus-evoked paradigm wherein acetone was applied to the left hindpaw during fMRI acquisition. In addition, we examined the time course of injury induced cold and mechanical hypersensitivity, as well as, anxiety-like behaviors, that coincided with early and late functional brain changes. Lastly, given recent evidence demonstrating SNI-induced morphometric changes in the ACC (Seminowicz et al., 2009) combined with evidence of altered glutamate and GABA signaling following induction of a neuropathic pain model (Bie et al., 2011; Gong et al., 2010; Li et al., 2014; Xu et al., 2008), we sought to assess whether early functional brain and behavioral changes associated with SNI and the development of cold hypersensitivity were related to local concentrations of glutamate (Glu) and/or GABA, or precursor molecules such as glutamine (Gln) and the glutamate/glutamine complex (Glx), in the ACC using in vivo ^{1}H magnetic resonance spectroscopy (MRS).

Materials & methods

Animals

12 adult female Sprague–Dawley rats (200–250 g, Charles River, CD; 6 weeks of age) were housed in ventilated plastic cages with soft bedding, and maintained on a 12/12 h light/dark cycle (lights on at 07:00), at constant temperature (22 ± 2 °C) and humidity (50 ± 10%). Rats were fed standard rat chow and had access to tap water ad libitum. All procedures were approved by the Institutional Animal Care and Use Committee at the University of Maryland and performed in accordance with the National Institutes of Health Guide for the Care and Use of Laboratory Animals.

Our rationale for choosing female rats was threefold: 1) in humans, females show a higher prevalence of chronic pain disorders (Craft et al., 2004; Fillingim and Ness, 2000), thus females seem to be more susceptible to developing chronic pain conditions than males, suggesting that hormonal influences may play an important role in the pathogenesis of chronic pain, 2) despite the higher prevalence of chronic pain disorders in females and numerous reports of sex differences in the neurobiology underlying nociceptive signaling and the subsequent experience of pain (Mogil, 2012; Paller et al., 2009), the majority of preclinical research has focused on elucidating pain circuitry in male rodents, therefore, more female rodent studies are needed to address this imbalance in the pain literature (Mogil and Chanda, 2005), and 3) conducting longitudinal neuroimaging studies in male rats becomes a technical constraint, since male rats undergo rapid growth spurts compared to females, and in some cases, the cranium exceeds the size of the head coil in older male rats.

Surgical procedures

Rats were randomly assigned to undergo SNI (n = 7) or sham (n = 5) surgery. Prior to surgery, each animal was anesthetized with a mixture of ketamine/xylazine (80/10 mg/kg, i.p. respectively). Once the animal was unresponsive to tail pinch, skin incision and blunt dissection through the left biceps femoris muscle was performed and a segment of the sciatic nerve was exposed between the mid-thigh and the popliteal fossa. For the SNI animals, the three major divisions of the sciatic nerve (common peroneal, tibial, and sural nerve) were separated based on individual perineuria. The common peroneal and tibial nerves were tightly ligated with a 6.0 silk suture and sectioned distal to the ligation, removing 1–2 mm of distal nerve stump, and leaving the sural nerve intact. Care was taken to avoid touching or stretching the intact sural nerve. For both SNI and sham rats, complete hemostasis was confirmed and topical lidocaine (Sparhawk Laboratories, Inc.) was applied to the skin and muscle around the wound prior to closure of incisions with the muscle (resorbable 4-0 sutures) and skin (4-0 silk) sutures. Rats were then placed on thermo-regulated heat pads and monitored until full recovery from anesthetic was achieved. Rats were returned to their home cages and monitored on a daily basis until wounds were completely healed.

Behavioral testing

All behavioral testing was conducted in a lit room between the hours of 08:30 and 14:00, 2 weeks prior to surgery (pre-injury) and 2, 5, 9, 14 and 19 weeks post-injury (Fig. 1). On each testing day, animals were acclimated to the testing environment for 30 min prior to commencement of behavioral experiments. Mechanical and cold sensitivity were assessed using the von Frey and acetone cold sensitivity test (CST). In addition, anxiety-like and exploratory behaviors were measured using the open field (OF) arena and elevated-plus maze (EPM) paradigms. Behavioral testing equipment was cleaned with 70% ethanol between animals. All rodent handling during behavioral experiments was conducted by a female researcher (C.S.H.) (Sorge et al., 2014).

Mechanical hypersensitivity was measured using the von Frey method adapted from Chaplan et al. (1994). Briefly, animals were first habituated to a 24.13 × 13.97 × 24.13 cm Plexiglas test chamber placed on top of a metal mesh screen for 10 min. Each animal was then tested to determine the 50% mechanical withdrawal thresholds for the left (ipsilateral to surgery) and right (contralateral to surgery) hindpaws using a modified up and down method (Chaplan et al., 1994). Eight calibrated von Frey monofilaments with ascending forces, ranging from 1 to 15 g (1, 1.4, 2, 4, 6, 8, 10, and 15) were used. Each trial began with a von Frey force of 1 g delivered in a perpendicular fashion to the lateral plantar surface of the left or right hindpaw for approximately 1–2 s. A positive response was operationally defined as a rapid withdrawal of the hindpaw, whereas a negative response was defined by the absence of a hindpaw flexion withdrawal reflex or ambulation. Two positive responses to the same mechanical probe were required to start the series. The 50% withdrawal thresholds for the ipsilateral and contralateral hindpaws were averaged separately across the six trials for each animal at each time point and then log transformed.

The acetone CST (Choi et al., 1994) was used to quantify differences in the development and maintenance of cold hypersensitivity in SNI compared to sham animals across the pre- and post-injury time points. Prior to the start of the experiment, each rat was placed in a Plexiglas test chamber on top of a metal mesh grid and allowed to acclimate for 10 min. Acetone delivery to the hindpaw was accomplished by forming an acetone bubble at the end of a piece of polyethylene (PE; inner diameter = 1.57 mm, Intramedic PE205, Becton Dickinson) tubing connected to a 1 ml male luer-tipped syringe. The acetone bubble was then gently applied to the plantar surface of the left or right hindpaw. Duration (s) of time spent lifting, shaking, or licking the left or right hindpaws were measured following each application. For each rat, there were a total of 6 trials in which acetone was applied to either the left or right hindpaw, with two min interstimulus intervals (ISI) between acetone applications. The stimulus parameters (i.e., number of trials, ISI) for the acetone CST during fMRI were identical to those in

Please cite this article as: Hubbard, C.S., et al., Behavioral, metabolic and functional brain changes in a rat model of chronic neuropathic pain: A longitudinal MRI study, NeuroImage (2014), http://dx.doi.org/10.1016/j.neuroimage.2014.12.024

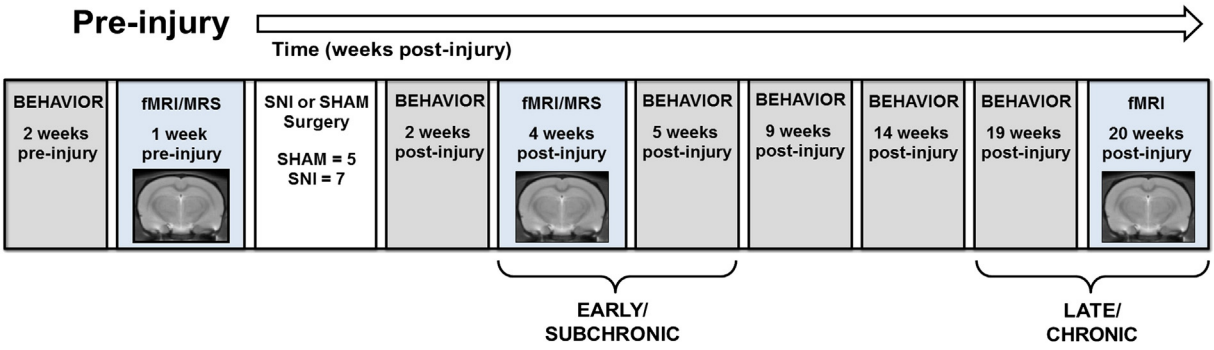

Fig. 1. Schematic illustrating the experimental design. All rats underwent behavioral testing (gray boxes) at six different time points, 2 weeks prior to SNI or sham surgery (pre-injury) and 2, 5, 9, 14, and 19 weeks following surgery (post-injury). On each behavioral testing day, mechanical and cold sensitivity were assessed using the von Frey and the acetone CST, respectively. Anxiety-like and exploratory type behaviors were also measured using the OF and EPM. fMRI scanning (blue boxes) during acetone application to the left hindpaw was conducted 1 week prior to surgery (pre-injury) and at 4 (early/subchronic) and 20 weeks (late/chronic) post-injury in order to examine the time course of functional brain changes associated with the development and maintenance of cold hypersensitivity following peripheral nerve damage. In addition, magnetic resonance spectroscopy (MRS) was performed following the fMRI scans at the pre-injury and 4 weeks post-injury scan time points to assess the relative concentrations of Glu, GABA, Gln, and Glx in the ACC in SNI rats compared to shams.

the behavioral sessions, with the exception that acetone was only applied to the left hindpaw in the fMRI experiments.

Anxiety-like behaviors were measured using OF and EPM paradigms. Behaviors were video recorded with a digital camera mounted above each apparatus and automatically coded using ANY-maze (version 4.96; Stoelting Co., IL) video tracking software. The OF arena consisted of a 44.45 × 44.45 × 30.48 cm Plexiglas enclosure with a black metal bottom and opaque sides. The arena was divided into a 5 × 5 grid of equally sized virtual squares (virtual square = 8.9 cm × 8.9 cm) superimposed onto video recordings with ANY-maze. The outer section of the arena was defined as the sum of all squares adjacent to a wall (i.e., 20 squares), whereas the central region consisted of a large center with 9 virtual squares. The experiment began with placement of a rat in the middle square of the large center. ANY-maze software automatically tracked and coded the number of line crossings and entries into the large center of the OF across a 5 min period. The criterion for entry into either the outer section or large center region was set to 80% of the animal's body in reference to its center point. The EPM was a cross-shaped platform consisting of 4 equally-sized arms (50.2 cm × 8.9 cm) elevated 70 cm above ground, with two arms flanked by 50.8 cm high opaque walls (closed arms) and two exposed arms with no walls (open arms), connected via a middle platform (8.9 cm × 8.9 cm). Virtual zones for the open and closed arms were created and superimposed onto video recordings using ANY-maze. At the start of the experiment a rat was placed in the middle platform, facing an open arm, and the number of total closed arm exits was recorded and automatically coded across a 5 min period. Exit from a closed arm required that 80% of the animal's body, in reference to its center point, was located outside the zone of interest (i.e., closed arm). Other indices of anxiety-like and avoidance/exploratory type behaviors, including the number of grooming bouts, corner-facing events, stretch-attend postures, and rearings, were coded blindly by an independent rater from video recordings for each OF and EPM experiment. The number of fecal pellets was also counted at the end of each OF and EPM experiment.

MRI and MRS data acquisition

Rats were scanned using a Bruker BioSpec 70/30 USR Avance III 7 T MRI scanner (Bruker Biospin MRI GmbH, Germany). The system was equipped with a BGA12S gradient system and interfaced to a Bruker Paravision 5.1 console. A Bruker 40 mm circular polarized volume coil was used for acquisition. In vivo MRI experiments were performed 1 week prior to (pre-injury scan) and 4 (early/subacute) and 20 weeks (late/chronic) following surgery (post-injury scans; Fig. 1). Just before scanning, each rat was anesthetized with ≤1.5% isoflurane. Isoflurane levels were maintained at the same concentrations throughout the scan session and respiration and heart rates were continuously monitored using a small animal monitoring and gating system with corresponding software (SA Instruments, Inc., Stony Brook, NY, USA). The body temperature was maintained at 36–37 °C, using a circulating warm water heater. A high resolution T_1-weighted image was obtained (RARE, TR = 2000 ms, TE = 14 ms, 256 × 256, in plane resolution = 100 μm, 24 axial slices, 1 mm slice thickness) for anatomical reference. Functional scans were acquired using a spin-echo echo-planar imaging (EPI) sequence (TR = 1500 ms, TE = 35.096 ms, 75 × 75, in plane resolution = 400 μm, 24 axial slices) during resting state (550 volumes; data to be published in a separate report) and the acetone application paradigm (520 volumes). The acetone application paradigm began with a 30 s rest period (i.e., baseline) followed by 6 trials wherein application of 50 μl of acetone was delivered per trial, via a 20 ft length of PE tubing (inner diameter = 1.57 mm, Intramedic PE205, Becton Dickinson) connected to a 500 μl microsyringe (81201, Hamilton syringe fitted with a 16 gauge male luer tip) housed inside the scanner console room, with the end of the tubing positioned just proximal to the left hindpaw of the rat. Prior to the start of the experiment, the PE tubing was filled with deionized water followed by 300 μl of acetone (179124, Sigma-Aldrich) which was bracketed between two air bubbles (30 μl of air per bubble). Following the onset of acetone application to the left hindpaw, a 2 min ISI period ensued. A second 30 s rest period was recorded just prior to the end of the scan session.

After the acetone application paradigm, in vivo high resolution ^{1}H MRS experiments were performed at the pre-injury and the 4 weeks post-injury scan time points (Fig. 1). The adjustments of all first- and second-order shims over the voxel of interest were accomplished with the FASTMAP procedure. A customized short-TE PRESS pulse sequence (TR/TE = 2500/10 ms, na = 356) (Xu et al., 2013) was used for MRS data acquisition with voxel centered on the ACC (3 × 3 × 3 mm). MRS quantification of metabolites of interest was based on frequency domain analysis using a "Linear Combination of Model spectra" (LCModel) (Provencher, 2001). Cramer–Rao lower bounds (CRLBs), as reported from the LCModel analysis, were used to assess the reliability of the major metabolites (Bolliger et al., 2013). Metabolites having CRLBs values less than 20% were further analyzed. The reference for determining metabolite concentration was the water signal, which was acquired from the same voxel. The metabolic profile was measured with the same parameters except the number of averages was set at 8. The results were normalized by the LCModel to the metabolite concentrations and expressed as micromoles per gram wet weight (μmol/g).

Please cite this article as: Hubbard, C.S., et al., Behavioral, metabolic and functional brain changes in a rat model of chronic neuropathic pain: A longitudinal MRI study, NeuroImage (2014), http://dx.doi.org/10.1016/j.neuroimage.2014.12.024

Behavioral analysis

All statistical behavioral analyses were conducted using SPSS (version 22). Analyses for log-transformed 50% mechanical withdrawal thresholds (g) and acetone CST response durations (s) were performed separately using a 2 Group (SNI, sham) × 2 Side (ipsilateral, contralateral) × 6 Time (2 weeks pre-injury, and 2, 5, 9, 14 and 19 weeks post-injury) repeated measures ANOVA. For the OF paradigm, separate two-way repeated measures ANOVAs (Group × Time) were performed on the number of line crossings and number of entries into the large center of the arena. A two-way (Group × Time) repeated measures ANOVA analysis was also performed on the number of closed arm exits obtained during the EPM paradigm. For both paradigms, other indices of anxiety-like (number of defecations, grooming bouts) and avoidance/exploratory type behaviors (number of corner-facing events, stretch-attend postures, rearings) were also analyzed using two-way (Group × Time) repeated measures ANOVAs. For all behavioral analyses, post-hoc comparisons were performed using 2-tailed t-tests.

fMRI preprocessing and statistical analyses

All image preprocessing and statistical analyses were conducted using SPM8 (http://www.fil.ion.ucl.ac.uk/spm/). The preprocessing pipeline included slice timing correction, realignment, normalization, and smoothing with a 1 mm FWHM Gaussian kernel. A study-specific template was created by coregistering and averaging high-resolution T_1-weighted images across all animals at a single time point (4 weeks post-injury) and interpolating to voxel sizes of 0.5 × 0.5 × 0.5 mm. All scans at each time point for each rat were coregistered and normalized to this template as described in a previous report (Seminowicz et al., 2012).

All fMRI scans during the acetone application paradigm were approximately 13 min in duration and included a 30 s rest period, six 2 min blocks consisting of a stimulus application (~4 s), stimulus response (12 s), and a post-stimulus response period (~65 s). The scan ended with an additional 30 s of rest. For the first-level analysis, the BOLD signal during the stimulus application period was modeled using the onsets and durations of acetone application to the left hindpaw. To detect signal changes in the BOLD activity in response to acetone application to the left hindpaw, the stimulus response period was also modeled using the average acetone response duration obtained from the behavioral CST experiments for the SNI group across the 5 post-injury time points (i.e., 11.23 s), rounded up to the next integer (i.e., 12 s). The time between the offset of the stimulus response period and the onset of the second 30 s rest period was modeled as the post-stimulus response period. Rest periods were not included in the model (implicit baseline). In addition, motion parameters were entered into the model as nuisance variables and time and dispersion derivatives were added as regressors. To quantify brain response to acetone application, β-contrast images were created for voxels whose activation increased or decreased in response to acetone application.

To assess longitudinal effects, the first-level β-contrast images representing stimulus-evoked brain responses for each of the three scan time points (pre-injury and 4 weeks and 20 weeks post-injury) were entered as dependent variables in the general linear model for each rat within each group. Second level analysis was conducted using a 2 Group (Sham, SNI) × 3 Time (pre-injury and 4 and 20 weeks post-injury) flexible factorial design with Group and Time specified as fixed factors. We examined the Group × Time interactions between BOLD responses at the early (4 weeks post-injury) and late (20 weeks post-injury) scan time points relative to the pre-injury scans in order to determine the temporal changes in brain function resulting from peripheral nerve injury and associated with the development (early) and chronification (late) of allodynic-like behaviors. A series of restricted region of interest (ROI) small volume analyses was performed in SPM8 with hand drawn ROIs created using Analysis of Functional NeuroImages software (AFNI; version 2; http://afni.nimh.nih.gov/afni/) and based on the Paxinos and Watson rat brain atlas (Paxinos and Watson, 2005). The ROIs consisted of pain-related brain areas, including the periaqueductal gray (PAG), the left and right thalamus, hippocampus (Hc), insula, prefrontal cortical regions including the cingulate and prelimbic (PrL) cortices, and primary (S1) and secondary (S2) somatosensory cortices (Fig. 2). The cingulate cortex was further subdivided into the anterior cingulate cortex (ACC) rostrally and the midcingulate cortex (MCC) caudally based on the cytoarchitectural designations used by Vogt and Paxinos in rats and mice (Vogt and Paxinos, 2014). Small volume corrections using random field theory were used for the voxel-wise ROI restricted analysis, with thresholds set to $p = 0.05$. To correct for multiple comparisons, we used AFNI's 3dClustSim which determined the minimum cluster size of contiguous voxels within each ROI required to reach significance at an alpha level of $p = 0.05$.

In addition, we extracted the parameter estimates for each significant cluster obtained from our ROI analyses across the three imaging time points (1 week pre-injury and 4 and 20 weeks post-injury) and calculated difference scores for each animal by subtracting the pre-injury scan time point from each of the post-injury time points. Difference scores for each animal were calculated in a similar manner for the acetone CST behavioral measure (left hindpaw response durations) using the 2 weeks pre-injury and 5 and 19 weeks post-injury time points. Difference scores for the parameter estimates and behavioral CST response durations at the early (~1 month) or late (~5 months) post-injury time points were then correlated using Pearson's R bivariate correlational analyses (2-tailed) in SPSS.

MRS analyses

To assess the relative concentrations of Glu, GABA, Gln and Glx, within the ACC in SNI rats compared to shams across the pre-injury and 4 weeks (early) post-injury scan time points, we conducted separate two-way repeated measures ANOVAs (Group × Time) on each metabolite using SPSS. In addition, we conducted exploratory analyses using two-way (Group × Time) repeated measures ANOVAs on other metabolites within the ACC, for which we had no *a priori* hypotheses, but which showed CRLBs values less than 20% according to the results from the LCModel analysis. These metabolites included *N*-acetylaspartate (NAA), total creatine (tCr), total choline (tCho), *myo*-inositol (MI), *N*-acetylaspartylglutamate (NAAG), glutathione (GSH) and taurine (Tau). Lastly, to assess if concentrations of Glu, GABA, Gln, or Glx, in the ACC were related to peripheral nerve injury induced changes in cold sensitivity, we performed Pearson's R bivariate correlational analyses on difference scores calculated from the acetone CST behavioral measure (left hindpaw response durations) and metabolite concentrations (in μmol/g wet weight) obtained at the pre- and post-injury time points for each group of rats separately. The difference scores for the acetone CST were calculated by subtracting the response durations (s) for the 2 weeks pre-injury time point from the 5 weeks post-injury time point, and correlating these with the difference scores calculated by subtracting the 1 week pre-injury MRS metabolite concentrations (i.e., Glu, GABA, Gln, and Glx) from the 4 weeks post-injury MRS metabolite concentrations.

Results

SNI-induced early and long-term mechanical and cold hypersensitivity

Results for the allodynia-like behavioral measures assessed during the von Frey and acetone CST tests are displayed in Fig. 3. For the von Frey test, analysis yielded a significant Group × Side ($F = 20.49$, $p = 0.001$) interaction, with SNI rats showing a significant decrease in withdrawal thresholds for the ipsilateral hindpaw compared to shams. In addition, a significant Group × Side × Time interaction ($F = 5.71$, $p = 0.028$) and a main effect of Side ($F = 19.88$, $p = 0.001$) were found.

Please cite this article as: Hubbard, C.S., et al., Behavioral, metabolic and functional brain changes in a rat model of chronic neuropathic pain: A longitudinal MRI study, NeuroImage (2014), http://dx.doi.org/10.1016/j.neuroimage.2014.12.024

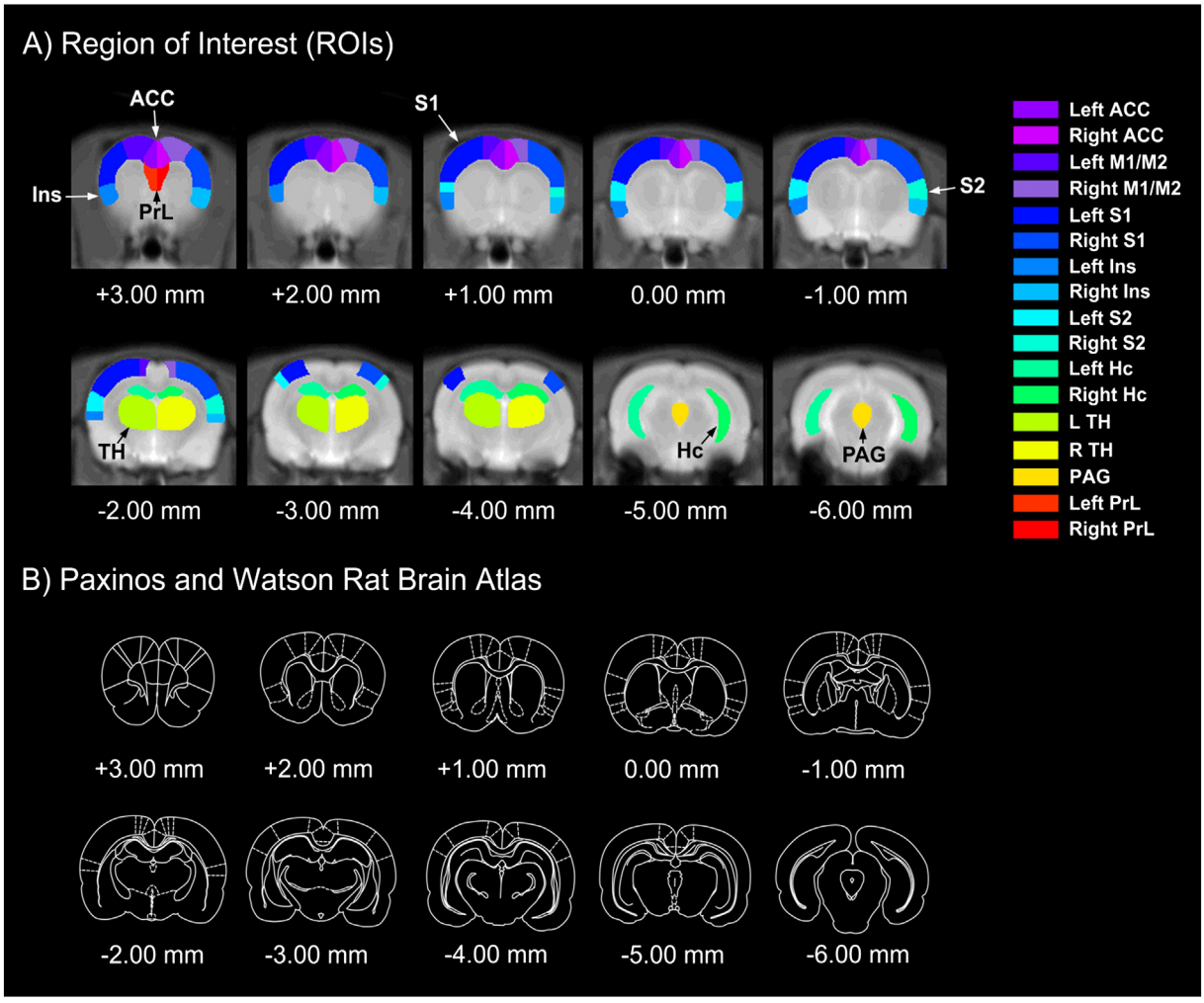

Fig. 2. Regions of interest (ROIs) used for the fMRI analysis. (A) ROIs were hand-drawn masks overlaid onto T_1-weighted averaged rat brain template images (1 mm slice thickness). ROIs were defined based on the closest approximation to the corresponding anatomical sections taken from the Paxinos and Watson stereotaxic rat brain atlas (Paxinos and Watson, 2005). ROIs are color-coded for display purposes and include the following left (L) or right (R) hemispheric structures: ACC, prelimbic cortex (PrL), insula (Ins), primary (S1) and secondary (S2) somatosensory cortices, thalamus (TH), hippocampus (Hc), and periaqueductal gray (PAG). Primary and secondary motor areas (M1/M2) are shown for anatomical reference, but were not included in the analysis. (B) Anatomical overlays taken from the Paxinos and Watson rat brain atlas depicting the corresponding anatomical sections for the ROI restricted fMRI analyses during topical application of acetone to the injured hindpaw (Paxinos and Watson, 2005).

Post-hoc tests (2-tailed t-tests) revealed that at the pre-injury time point, groups did not differ in their withdrawal response thresholds for the ipsilateral hindpaw ($p = 0.60$; Fig. 3A). However, at 5, 9, 14 and 19 weeks post-injury relative to the pre-injury time point, SNI rats showed significantly lower withdrawal thresholds for the ipsilateral hindpaw (p's ≤ 0.001; Fig. 3A). No significant group differences were observed across the pre- and post-injury time points for the contralateral hindpaw (p's ≥ 0.22; Fig. 3B). For the acetone CST, analysis revealed significant Group × Side ($F = 42.388$, $p < 0.001$) and Group × Side × Time ($F = 24.76$, $p = 0.001$) interactions, as well as main effects of Time ($F = 15.20$, $p = 0.002$) and Side ($F = 30.41$, $p < 0.001$). Post-hoc tests (2-tailed t-tests) showed no significant group difference in acetone response durations at the pre-injury time point ($p = 0.42$) for the ipsilateral hindpaw (Fig. 3C). However, at 2, 5, 9, 14 and 19 weeks post-injury SNI rats showed significantly greater response durations (s) following acetone application to the ipsilateral (p's ≤ 0.017; Fig. 3C), but not the contralateral hindpaw compared to shams (p's ≥ 0.056; Fig. 3D). In addition, within-subjects comparisons revealed a significant decrease in CST response duration for the left hindpaw in SNI rats at 19 compared to 14 weeks post-surgery ($p = 0.024$). No other significant differences between post-surgery time points were found in SNI rats nor in the sham control group. Results from the von Frey and acetone CST revealed significant early and sustained increases in mechanical and cold sensitivity in SNI rats compared to shams, a finding which is consistent with results from previous studies (Choi et al., 1994; Low et al., 2012; Seminowicz et al., 2009).

SNI had no effect on anxiety-like or exploratory behaviors

Results for the anxiety-like behavioral measures assessed during the OF and EPM are displayed in Fig. 3. The repeated measures ANOVA analysis for the number of line crossings obtained during the OF revealed a significant Group × Time interaction ($F = 4.59$, $p = 0.045$), however p-values derived from the post-hoc tests (i.e., 2-tailed t-tests) did not reach significance for any of the pre- versus post-injury contrasts (p's ≥ 0.174; Fig. 3E). In addition, no significant main effects or interactions were observed for the number of entries into the large center of the OF arena (p's > 0.752), nor were there any significant main effects for Time or Group × Time interactions for number of corner-facing events, stretch-attend postures, rearings, grooming bouts, or defecations. Results did reveal a significant main effect of Time ($F = 6.65$, $p = 0.02$) for the number of grooming bouts during the OF test. Both groups of rats showed significant decreases in grooming behaviors at 4 weeks post-injury versus pre-injury ($p = 0.005$), likely due to habituation to the OF arena. Overall, our results indicate that peripheral nerve injury had no effect on anxiety-like or exploratory behaviors measured

Please cite this article as: Hubbard, C.S., et al., Behavioral, metabolic and functional brain changes in a rat model of chronic neuropathic pain: A longitudinal MRI study, NeuroImage (2014), http://dx.doi.org/10.1016/j.neuroimage.2014.12.024

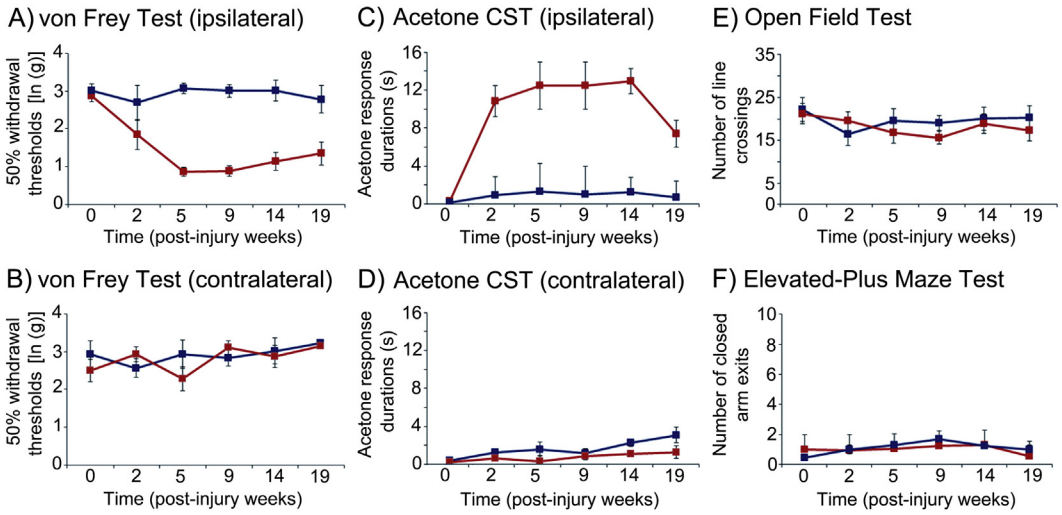

Fig. 3. Line graphs depicting the means and standard errors for the allodynic- and anxiety-like behavioral measures across the pre-injury and post-injury time points for SNI (red lines) and sham (blue lines) rats. For the behavioral measure of mechanical sensitivity assessed using the von Frey test, groups did not differ in their log transformed 50% withdrawal response thresholds for the (A) left (ipsilateral to the side of surgery) or (B) right (contralateral to the side of surgery) hindpaws at the pre-injury time point. At 5, 9, 14, and 19 weeks post-injury, SNI rats showed significantly lower withdrawal response thresholds for the ipsilateral (p's ≤ 0.001), but not contralateral, hindpaw compared to shams. No significant group differences in withdrawal response thresholds were observed across the pre- versus 2 weeks post-injury time points for either the ipsilateral or contralateral hindpaw. For the behavioral measure of cold sensitivity assessed during the acetone cold sensitivity test (CST) at 2, 5, 9, 14, and 19 weeks post-injury relative to baseline, SNI rats showed significantly greater response durations (s) following acetone application to the (C) ipsilateral hindpaw, but not (D) contralaterally, compared to shams. Groups did not differ in acetone response durations at the pre-injury time point for either the ipsilateral or contralateral paw. No significant group differences in anxiety-like behaviors assessed by the number of line crossings during the open field (E) or the number of closed arm exits during the elevated plus maze (F) across the pre-injury and post-injury time points were found.

during the OF test. For the EPM (Fig. 3F), there was a significant main effect of Time ($F = 13.43$, $p = 0.003$), such that rats in both groups showed increases in the number of closed arm exits at 9 weeks post-injury ($p = 0.026$; Fig. 3F) relative to the pre-injury time point. However, no Time × Group interaction ($F = 1.57$, $p = 0.299$) was observed for the number of closed arm exits, indicating that peripheral nerve injury had no effect on this measure of anxiety-like behavior. We also found no significant group differences in the number of corner-facing events, stretch-attend postures, rearings, or grooming bouts. Moreover, we observed no defecations in either group of rats across any of the six behavioral time points. In summary, SNI rats showed no signs of anxiety-like behaviors at any of the time points tested during either the OF or EPM paradigms.

Whole-brain and ROI-restricted analyses

Whole-brain analysis yielded widespread early and late functional brain changes in SNI rats. At the early post-injury time point relative to baseline, acetone application to the left hindpaw induced greater activation in SNI rats compared to shams in brain areas involved in pain processing such as the contralateral somatosensory cortex, VPL of the thalamus, and dorsal striatum. In addition, larger deactivations were observed in areas involved in processing the affective-motivational aspects of pain including the contralateral insula, medial thalamus, and ipsilateral ACC. Interestingly, midbrain and brainstem regions such as the PAG and pontine nuclei also showed greater deactivations in SNI rats compared to shams. At the late post-injury time point relative to baseline, SNI rats showed greater stimulus-evoked activations in the ACC and prelimbic region, insula, basal ganglia, and somatosensory cortices, whereas marked and sustained deactivations were seen in the medial thalamus and PAG.

Based on our *a priori* hypotheses, we conducted a series of ROI restricted analyses to characterize the early and long-term effects of peripheral nerve injury on functional brain changes in pain-related areas evoked by acetone application to the left hindpaw in SNI rats compared to sham controls (see below). Inline Supplementary Fig. S1 illustrates the mean (± SEM) parameter estimates at 4 and 20 weeks post-injury versus baseline (post–pre) for the major findings obtained from our ROI analyses for each group (see Inline Supplementary Fig. S1).

Inline Supplementary Fig. S1 can be found online at http://dx.doi.org/10.1016/j.neuroimage.2014.12.024.

SNI-induced early functional brain changes in response to innocuous cold stimuli

Fig. 4 displays the parametric maps for the whole-brain and ROI-restricted between group analyses for the acetone application fMRI paradigm at the early (4 weeks; A–B) and late (20 weeks; C–D) post-injury time points. Table 1 shows the corresponding peak voxel T- and p-values for the significant clusters obtained from the restricted ROI analysis. At 4 weeks post-injury (Table 1, Fig. 4B), SNI rats showed significantly greater BOLD activation compared to shams contralateral to

Fig. 4. Results from the whole-brain and region of interest (ROI) restricted analyses for the acetone application paradigm at the early (4 weeks) and late (20 weeks) post-injury time points. (A) Whole-brain activation and deactivation T maps displaying blood-oxygen-level dependent (BOLD) signal changes for the SNI > sham (activations; warm voxels) and SNI < sham (deactivations; cool voxels) contrasts at 4 weeks post-injury versus baseline (4 weeks post-injury > pre-injury). (B) ROI restricted activation and deactivation T maps displaying BOLD signal changes for the SNI > sham (activations; warm voxels) and SNI < sham (deactivations; cool voxels) contrasts at the 4 weeks post-injury versus baseline (4 weeks post-injury > pre-injury). For the ROI restricted analysis, cluster thresholds were corrected for multiple comparisons using AFNI's 3dClustSim which determined the minimum cluster size of continuous voxels within each ROI to reach significance at an alpha level of $p = 0.05$. (C) Whole-brain activation and deactivation T maps displaying blood-oxygen-level dependent (BOLD) signal changes for the SNI > sham (activations; warm voxels) and SNI < sham (deactivations; cool voxels) contrasts at 20 weeks post-injury versus baseline (20 weeks post-injury > pre-injury). (D) ROI restricted activation and deactivation T maps displaying BOLD signal changes for the SNI > sham (activations; warm voxels) and SNI < sham (deactivations; cool voxels) contrasts at the 20 weeks post-injury versus baseline (20 weeks post-injury > pre-injury). For the ROI restricted analysis, cluster thresholds were corrected for multiple comparisons using AFNI's 3dClustSim which determined the minimum cluster size of continuous voxels within each ROI to reach significance at an alpha level of $p = 0.05$. Abbreviations: ACC = anterior cingulate cortex; ACC/PrL = anterior cingulate/prelimbic cortex; Hc = hippocampus; Ins = insula; PAG = periaqueductal gray; S1 = primary somatosensory cortex; S2 = secondary somatosensory cortex; TH = thalamus; L = left; R = right.

Please cite this article as: Hubbard, C.S., et al., Behavioral, metabolic and functional brain changes in a rat model of chronic neuropathic pain: A longitudinal MRI study, NeuroImage (2014), http://dx.doi.org/10.1016/j.neuroimage.2014.12.024

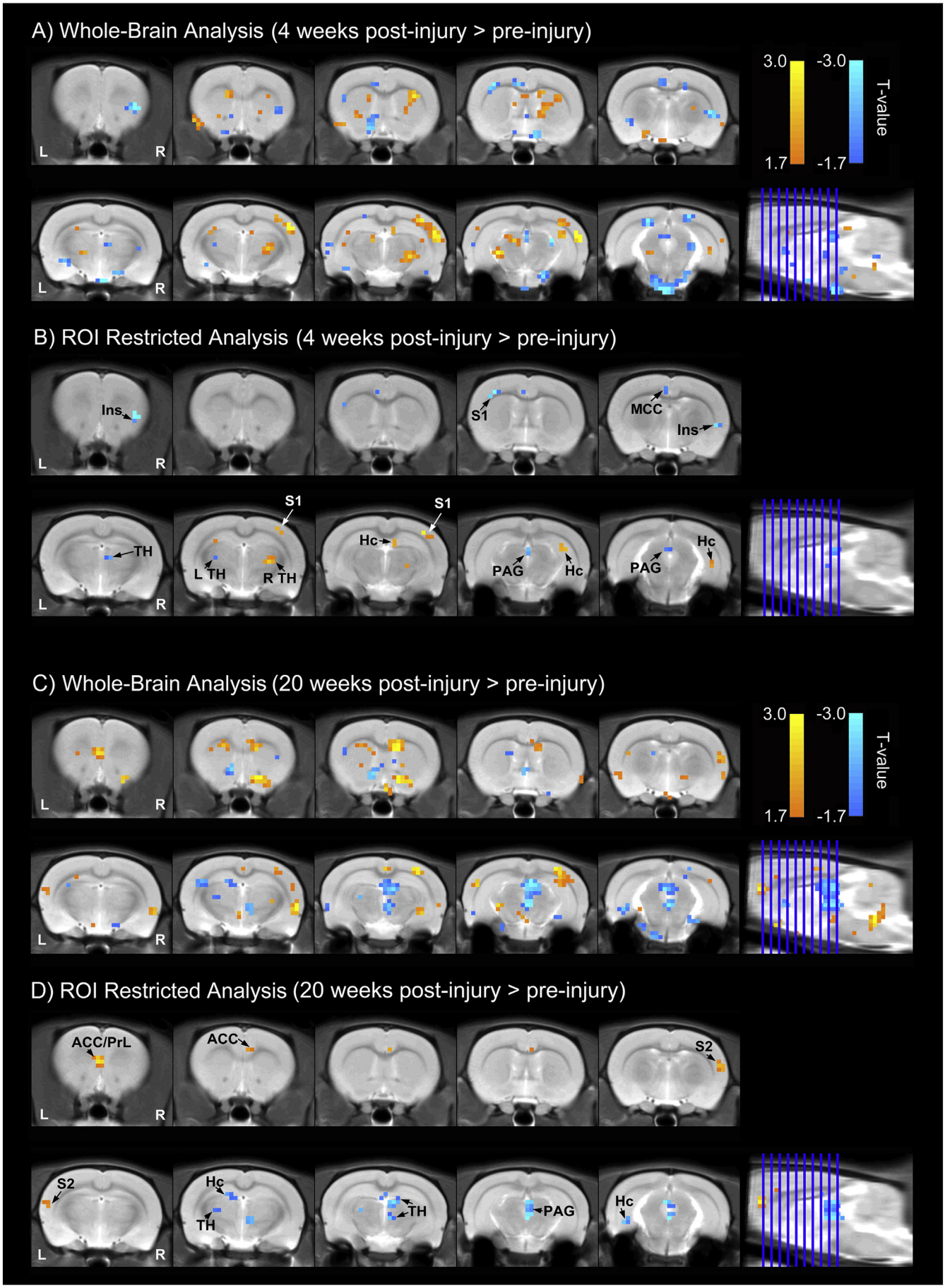

Please cite this article as: Hubbard, C.S., et al., Behavioral, metabolic and functional brain changes in a rat model of chronic neuropathic pain: A longitudinal MRI study, NeuroImage (2014), http://dx.doi.org/10.1016/j.neuroimage.2014.12.024

the side of injury, in the right ventroposterior lateral (VPL) nucleus of the thalamus and right S1. SNI rats also showed relatively greater bilateral activation in the Hc compared to shams. Significant decreases in BOLD activity contralateral to the side of injury were also observed in the right medial thalamus and two clusters in the right insula, one located rostrally and the other caudally. Ipsilateral to the side of injury, relative decreases were seen in the left ACC and midcingulate (MCC) cortices, as well as the left VPL, and left S1. In addition, SNI rats showed significant deactivation in the PAG compared to shams. Inline Supplementary Fig. S1 displays the mean (± SEM) parameter estimates at 4 weeks post-injury versus pre-injury time points (post – pre) for the major significant clusters obtained from our ROI analyses for each group.

SNI-induced late functional brain changes in response to innocuous cold stimuli

At 20 weeks post-injury relative to baseline (Table 1 and Fig. 4D), SNI rats showed significantly greater bilateral activations in S2 relative to sham controls. In contrast to the deactivation observed in the left ACC at 4 weeks post-injury, at 20 weeks post-injury, SNI rats showed significantly greater activation in more anterior regions of the left ACC, encompassing the PrL. SNI rats also showed a significant increase in BOLD activity in the right MCC relative to shams. Consistent with findings at 4 weeks post-injury, at 20 weeks SNI rats relative to shams showed significant deactivations in the PAG, left VPL, and two right medial thalamus clusters. The two clusters in the medial thalamus were situated along the dorsal and ventral aspects of the midline thalamic nuclei (Fig. 4D). SNI rats also showed a significant decrease in BOLD activity in the left Hc compared to shams at 20 weeks post-injury.

SNI-induced late functional brain changes in the anterior cingulate and prelimbic cortices associated with cold hypersensitivity

In SNI rats, correlational analysis between the acetone CST response durations and BOLD signal changes for significant clusters extracted from the ROI restricted analysis during acetone application at the early post-injury time point (~1 month) revealed only a positive trend (i.e., increased cold sensitivity associated with increased BOLD activity changes) in the right caudally-located insular cluster ($r = 0.708$, $p = 0.075$). In the sham group, we found a significant negative correlation between acetone CST response durations and BOLD signal changes in the left S1 ($r = -0.955$, $p = 0.012$; Fig. 5A) and in the right VPL of the thalamus ($r = -0.877$, $p = 0.051$). At the late post-injury time point (~5 months), correlational analyses between acetone response durations and BOLD signal changes revealed a significant positive correlation in SNI rats for the left ACC/PrL region ($r = 0.80$, $p = 0.022$; Fig. 5B), with a correlation approaching significance for the right S2 ($r = 0.698$, $p = 0.081$). A significant positive correlation between response durations and BOLD signal changes in the left ACC/PrL ($r = 0.955$, $p = 0.011$; Fig. 5B) was also found for shams, however, the magnitude of change in SNI rats was much larger compared to shams indicating that greater activity in the ACC/PrL was associated with greater cold sensitivity in these animals.

SNI-induced increases in glutamate in the anterior cingulate cortex associated with cold hypersensitivity

A summary of the MRS results is displayed in Fig. 6A. Figs. 6B and C depict the ACC region of interest for in vivo ^{1}H MRS scanning and a representative spectrum at the pre-injury scan time point. Repeated measures ANOVAs revealed trends toward a significant main effect of Time ($F = 4.82$, $p = 0.053$) and Group × Time interaction for Glu ($F = 4.88$, $p = 0.052$). At the early post-injury time point, SNI rats compared to shams showed increased levels of Glu in the ACC (Fig. 6A). There were no significant main effects or Group × Time interactions for GABA (p's > 0.848) or Gln (p's > 0.537), although a trend toward a significant main effect for Time ($p = 0.072$) appeared for the Glx, with rats showing increased Glx concentrations at 4 weeks post-injury relative to baseline (Fig. 6A). In addition, there were main effects for Time for NAA ($p = 0.051$) and Tau ($p = 0.020$). Both SNI and sham rats showed significant increases in *N*-acetylaspartate (NAA) and significant decreases in Tau at 4 weeks post-injury compared to the pre-injury time point. Altered concentrations of NAA and Tau in the ACC in both groups of rats at 4 weeks post-surgery likely reflect age-related changes associated with neocortical development (Angelie et al., 2001; Bluml et al., 2013; Paban et al., 2010; Zhang et al., 2009).

Correlational analyses with difference scores for the post- minus pre-injury time points for the behavioral CST scores and concentrations of Glu, GABA, Gln, and Glx, revealed significant positive relationships for Glu ($r = 0.782$, $p = 0.038$; Fig. 6D) and Glx ($r = 0.872$, $p = 0.010$; Fig. 6E) for the SNI group, but not shams (p's > 0.253). These results suggest that the development of cold hypersensitivity due to peripheral nerve damage was associated with increased levels of both Glu and Glx concentrations in the ACC at 4 weeks post-injury.

Discussion

The present study examined the time course of SNI-induced functional brain changes associated with the development and maintenance of cold hypersensitivity in female rats, using a novel, chronic neuropathic pain model of cold allodynia during fMRI. SNI rats showed early (subchronic) and late (chronic) functional brain changes associated with acetone application in areas important for processing the affective-

Table 1
Summary of Group × Time interactions for the restricted ROI analysis.

Contrast	4 weeks post-injury > pre-injury				20 weeks post-injury > pre-injury			
	Region	Cluster size	Peak T-value	Peak *p*-value	Region	Cluster size	Peak T-value	Peak *p*-value
SNI > sham	R TH (VPL)	14	2.50	0.009	L S2	3	2.01	0.026
	R S1	8	2.79	0.005	R S2	9	2.33	0.013
	L Hc	4	2.18	0.019	L ACC/PrL	14	3.63	0.001
	R Hc (rostral)	8	2.71	0.005	R MCC	7	2.23	0.017
	R Hc (caudal)	7	2.35	0.012				
SNI < sham	L TH (VPL)	5	−2.14	0.020	L TH (VPL)	5	−2.37	0.012
	R mTH	4	−2.26	0.016	R mTH (dorsal)	9	−2.92	0.003
	L S1	6	−2.97	0.003	R mTH (ventral)	9	−2.79	0.005
	L ACC/MCC	4	−2.15	0.020	L Hc	6	−2.58	0.007
	PAG	7	−2.50	0.009	PAG	36	−3.00	0.003
	R Ins (rostral)	6	−3.54	0.001				
	R Ins (caudal)	4	−2.70	0.006				

Peak voxels in significant clusters for the left (L) or right (R) restricted region of interest (ROI) analyses at 4 weeks (early) and 20 weeks (late) post-injury relative to the pre-injury time point. Abbreviations: thalamus (TH), ventroposterior lateral (VPL) nucleus of the TH, medial TH (mTH), primary (S1) and secondary (S2) somatosensory cortices, hippocampus (Hc), anterior cingulate cortex (ACC), midcingulate cortex (MCC), prelimbic cortex (PrL), periaqueductal gray (PAG), and insula (Ins).

Please cite this article as: Hubbard, C.S., et al., Behavioral, metabolic and functional brain changes in a rat model of chronic neuropathic pain: A longitudinal MRI study, NeuroImage (2014), http://dx.doi.org/10.1016/j.neuroimage.2014.12.024

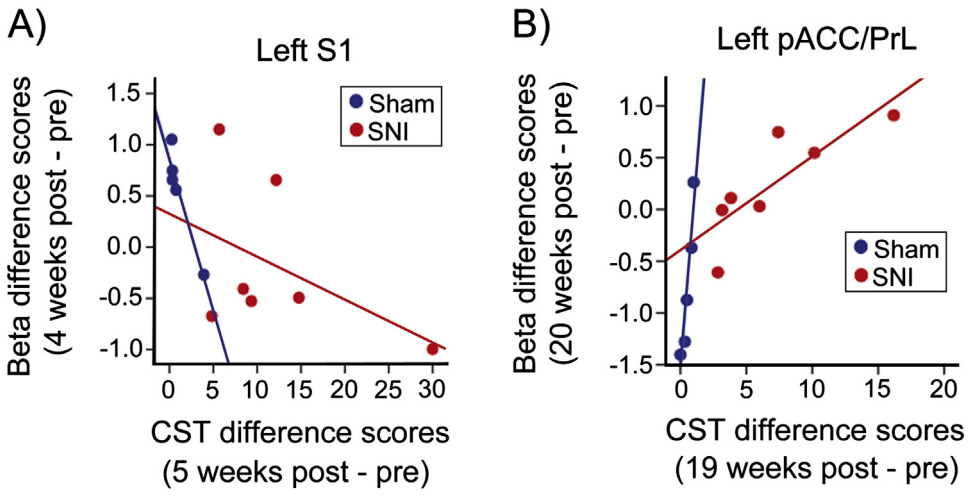

Fig. 5. Scatterplots displaying correlations between BOLD signal changes and magnitude changes in response durations during the behavioral acetone cold sensitivity test (CST) for SNI rats (red dots) and sham controls (blue dots) at the early (A) and late (B) time points. (A) At the early time point, approximately 1 month post-injury (weeks 4 and 5), analysis revealed a significant negative correlation between BOLD signal changes in the left S1 and the magnitude of change in CST response durations in shams, but not SNI rats. (B) At the late time point, approximately 5 months post-injury (weeks 19 and 20), positive correlations were found between BOLD signal changes in the left ACC/prelimbic (PrL) region and magnitude changes in CST response durations in both SNI rats and shams.

motivational and sensory-discriminative components of pain, including the ACC, VPL, and somatosensory cortices, as well as areas involved in the descending modulation of afferent nociceptive signaling, including midline thalamic nuclei and the PAG. The time course of these functional brain changes varied across the 5 month post-injury period, with some activation and deactivation patterns persisting (present at both early and late time points) and other transient changes, present at early or late time points. In SNI rats, these functional brain changes were associated with early and sustained increases in behavioral measures of mechanical and cold sensitivity. We also observed late activations in the ACC and PrL that were associated with larger magnitude increases in cold sensitivity in SNI rats relative to shams. SNI rats also showed early Glu increases in the ACC which correlated with cold hypersensitivity. Taken together, our findings indicate that peripheral nerve injury induces marked functional and metabolic brain changes that are accompanied by allodynic-like behaviors which persist for many months following injury. The time course associated with these neuroplastic and behavioral changes may reflect the chronification of neuropathic pain and the development of allodynic-like symptoms over prolonged periods of time.

Consistent with previous work, SNI induced rapid and long lasting mechanical and cold hypersensitivity (Decosterd and Woolf, 2000; Low et al., 2012; Sandkuhler, 2009; Seminowicz et al., 2009). However, SNI did not affect anxiety-like behaviors at any of the post-injury time points. These results are contrary to our hypothesis, and could be attributed to differences in methodological design, environmental factors, apparatus used, rodent strain, age, and/or sex of the animals (Kokras and Dalla, 2014; Kontinen et al., 1999; Leite-Almeida et al., 2009; Pritchard et al., 2013; Schmitt and Hiemke, 1998; Walsh and Cummins, 1976). The possibility of sex accounting for the different findings across studies is especially relevant given that the majority of studies used male rodents whereas females were used here. Indeed, sex differences using the OF and EPM have been described, with female rodents generally displaying less anxiety-like behaviors and increased exploration than their male counterparts (An et al., 2011; Frye et al., 2000; Johnston and File, 1991; Rodgers and Cole, 1993; Zimmerberg and Farley, 1993). Both SNI and sham rats showed significant decreases in the number of grooming bouts in the OF at 4 weeks post-injury versus baseline, further indicating that by the second time point our female rats had habituated to the OF and were not showing signs of stress or anxiogenic behaviors. Nevertheless, our data confirm previous findings demonstrating SNI-induced hypersensitivity to innocuous mechanical and cold stimuli which appear early, and persist over long periods of time, and further bolsters the utility of SNI as a model of chronic neuropathic pain in humans.

SNI induced early increased activity in the contralateral S1 and VPL, whereas ipsilaterally, early and sustained decreases were seen. These findings parallel previous results demonstrating abnormal thalamocortical connectivity between the VPL and S1 following spinal cord injury (Seminowicz et al., 2012). SNI rats also showed transient decreases in the right insula, at 4 weeks post-injury, which was absent by the late time point. Conversely, early activations were observed bilaterally in the hippocampus followed by late decreases ipsilaterally. In addition, we observed late bilateral S2 activation in SNI rats relative to shams. The aforementioned findings are largely in agreement with prior neuroimaging studies in humans with various chronic pain conditions and in rodent models of neuropathic pain demonstrating functional and structural abnormalities in pain-related brain regions such as the thalamus, insula, hippocampus, S1 and bilateral S2 (Apkarian et al., 2004; Baliki et al., 2012; Khan et al., 2014; May, 2008; Mutso et al., 2012; Seminowicz et al., 2009, 2012; Thompson and Bushnell, 2012).

A major finding in the current study was that SNI rats showed early and sustained decreases in key components of the descending pain modulatory system, including the contralateral midline thalamic nuclei and the PAG. The PAG has been implicated in the descending modulatory control of afferent nociceptive signaling as well as in the generation of defense-related behaviors (i.e., avoidance learning) (Stamford, 1995; Tang et al., 2009). The PAG sends ascending inhibitory projections to medial thalamic nuclei and in turn, receives descending excitatory projections from these nuclei, as well as from the ACC (Andersen, 1986; Mantyh, 1982; Marchand and Hagino, 1983; Sakata et al., 1988). Additionally, the PAG exerts descending inhibitory actions on medullary and spinal cord dorsal horn neurons, and electrical stimulation or opioid injection into the ventrolateral or dorsal PAG has profound analgesic effects (Mayer and Liebeskind, 1974; Reynolds, 1969; Yaksh et al., 1988). Since both ascending inputs from the PAG to the medial thalamus and descending pathways to the hindbrain and spinal cord are largely antinociceptive, it seems reasonable in light of our behavioral findings that the sustained decrease in the contralateral midline thalamic nuclei and PAG, combined with the concomitant late increase in ACC activity, may reflect disruptions in descending inhibition from the PAG and/or increased facilitation to this region, resulting in increased nociceptive afferent signaling (i.e., central sensitization) and the development and maintenance of neuropathic pain-like behaviors to an innocuous cold stimulus (Leith et al., 2010). These findings have important clinical and

Please cite this article as: Hubbard, C.S., et al., Behavioral, metabolic and functional brain changes in a rat model of chronic neuropathic pain: A longitudinal MRI study, NeuroImage (2014), http://dx.doi.org/10.1016/j.neuroimage.2014.12.024

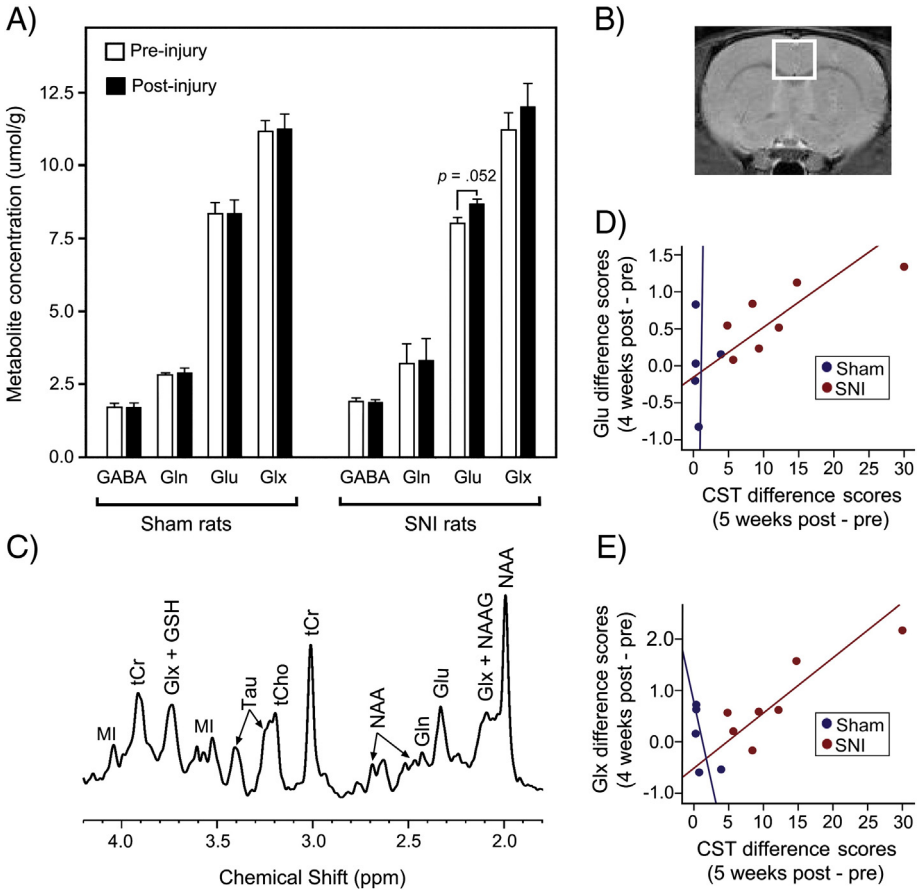

Fig. 6. Results from in vivo ^{1}H magnetic resonance spectroscopy (MRS) of the ACC. (A) Bar graph displaying the means and standard errors for metabolite concentrations (μmol/g wet weight) of glutamate (Glu), GABA, glutamine (Gln), and glutamate–glutamine complex (Glx), in SNI rats and shams at 4 weeks post-injury (black bars) relative to baseline (white bars; 1 week pre-injury). SNI rats, compared to shams, showed increased levels of Glu in the ACC 4 weeks post-injury relative to baseline. (B) The proton-density-weighted image of a coronal slice of a rat brain, in vivo, illustrates the rostral section of the ACC region of interest ($3 \times 3 \times 3$ mm^3) for MRS scanning. (C) Representative in vivo ^{1}H MR spectrum at 7 T during a baseline scan (pre-injury). The signals assigned in the spectra refer to the following metabolites: Glu, GABA, Gln, Glx, glutathione (GSH), total choline (tCho), *myo*-inositol (MI), *N*-acetylaspartate (NAA), *N*-acetylaspartylglutamate (NAAG), total creatine (tCr), and taurine (Tau). Scatterplots depicting positive correlations between magnitude changes in the concentration levels of Glu (D) and Glx (E) in the ACC and magnitude changes in CST response durations in SNI rats, but not shams.

research implications in that we show for the first time that chronic neuropathic pain induced by peripheral nerve injury produced marked and long-lasting changes in PAG functioning which likely reflect changes in PAG circuitry and closely resemble clinical manifestations of cold allodynia in humans suffering from various chronic pain conditions including peripheral neuropathy.

Another novel finding was that SNI rats showed early decreases in the left ACC/MCC followed by late increases in both the left ACC/PrL and right MCC. Converging evidence from human and animal studies suggest that the ACC is involved in processing cognitive, affective, and autonomic responses to pain and its anticipation, whereas the MCC is more involved in sensorimotor functions related to the motivational and goal-orientated aspects of the pain experience (Vogt et al., 1992; Vogt and Sikes, 2000). Thus, the reversal in activity in the left ACC/MCC at the late post-injury time point, along with the enhanced activation in the right MCC and the PrL, may reflect injury-induced maladaptive brain changes and subsequent functional cortical reorganization in areas important for processing the cognitive-evaluative and affective-motivational aspects of pain (Davis et al., 2011; Hashmi et al., 2013; Vertes, 2006). Furthermore, at the late post-injury time point, we observed greater BOLD signal in SNI than sham rats in the left ACC/PrL and activity in that region was positively correlated with cold hypersensitivity, indicating that peripheral nerve injury induced a greater degree of cold sensitivity, and that this cold allodynia was temporally related to the change in ACC activity.

Another important finding was that SNI rats showed increased Glu in the ACC compared to shams at the early post-injury time point. Glu is the primary excitatory neurotransmitter in the mammalian brain and is widely expressed throughout pyramidal neurons and glial cells in the neocortex (Erecinska and Silver, 1990). The early increase in Glu in the present study is in accordance with previous work demonstrating increased ^{1}H-MRS Glu concentrations in the ACC in humans during a pain-eliciting stimulus (Mullins et al., 2005) and enhanced presynaptic glutamatergic release, post-synaptic AMPA-receptor mediated responses, and NR2B-selective NMDA receptor overexpression, in the ACC in neuropathic or inflammatory pain models (Cao et al., 2009; Wu et al., 2005; Xu et al., 2008; Zhao et al., 2006). In addition, increased concentrations of Glu in the ACC, as well as Glx, were significantly correlated with the magnitude of cold hypersensitivity in SNI rats, suggesting that these behavioral changes may be related to increased glutamatergic neurotransmission and/or up-regulation in Glu–Gln cycling. Alternatively, changes in re-uptake mechanisms and/or increased degradation of glia may also be contributing factors. The role of glial cells in the development and maintenance of chronic neuropathic pain following peripheral nerve damage is well-established (Mika et al., 2013; Zhuo et al., 2011). We found no differences in MI, a putative marker of gliosis (Ross et al., 1998), between our SNI and sham rats, but given that MI is a marker of astrocyte activation, it remains possible that the changes observed here were due to migroglia. Another possibility is a loss of inhibition in ACC circuitry via disrupted GABAergic neurotransmission, which has also been implicated in the pathophysiology of chronic neuropathic pain. Disinhibition of GABA neurons in the ACC, in turn, might lead to hyperexcitability in nearby pyramidal neurons

(Blom et al., 2014). This hypothesis is partially supported by our fMRI results. At the early post-injury time point, SNI rats displayed greater BOLD decreases in the left ACC which were followed by a late reversal in activity, a finding which may reflect a loss of inhibitory drive over time and heightened cortical excitability.

Limitations

One potential limitation in the present study is that animals were anesthetized with isoflurane (≤1.5%) during the fMRI paradigm. Our rationale for using isoflurane was based on previous findings from rodent neuroimaging studies demonstrating intact stimulus-evoked BOLD signal responses, as well as spontaneous BOLD signal fluctuations during resting-state, using similar levels of sedation required to achieve immobility during scanning (Liu et al., 2004, 2013; Masamoto et al., 2007). Regardless, caution is needed when interpreting fMRI results in anesthetized animals even at the low levels of sedation used in the present study. The use of anesthetics in rodent neuroimaging and the inherent limitations have been extensively discussed elsewhere (Borsook and Becerra, 2011; D'Souza et al., 2014; Thompson and Bushnell, 2012).

Conclusion

The acetone application fMRI paradigm presented here represents a novel method for studying altered pain-related brain circuitry in a rat model of chronic neuropathic pain. Our results indicate that peripheral nerve injury induced functional and metabolic brain changes over extended periods of time that coincided with the development and maintenance of allodynic-like behaviors, including cold and mechanical hypersensitivity. This extensive functional and metabolic reorganization in pain-related brain circuitry particularly involving early hyperactivity of sensory areas (VPL, S1) and later hyperactivity of affective areas (ACC/PrL), and early and sustained hypoactivity of the medial thalamus and PAG, may reflect a progression from an acute and adaptive pain state to a chronic, maladaptive neuropathic disease state. Future work is needed to determine if the maintenance of cold and mechanical hypersensitivity can be prevented or reversed by blocking the functional and metabolic changes in regions identified in this study.

Acknowledgments

This research was supported by the Future Leaders in Pain Research Grant awarded by the American Pain Society (to D.A.S.) and funds provided by the Department of Neural and Pain Sciences, School of Dentistry, University of Maryland, Baltimore (to D.A.S.). We thank Dr. Rao Gullapalli, Steven Roys, Wenjun Zhu, and Andrew Marshall for their technical assistance with MRI and MRS parameter optimization and data acquisition. We would also like to thank Yadong Ji and Dr. Li Jiang for their assistance with rat surgical procedures and ROI analysis, Andrew Furman and Michael Keaser for their statistical advice, and Emily Peet for her assistance with behavioral coding. The authors declare no competing financial interests.

References

An, X.L., Zou, J.X., Wu, R.Y., Yang, Y., Tai, F.D., Zeng, S.Y., Jia, R., Zhang, X., Liu, E.Q., Broders, H., 2011. Strain and sex differences in anxiety-like and social behaviors in C57BL/6J and BALB/cJ mice. Exp. Anim. 60, 111–123.

Andersen, E., 1986. Periaqueductal gray and cerebral cortex modulate responses of medial thalamic neurons to noxious stimulation. Brain Res. 375, 30–36.

Angelie, E., Bonmartin, A., Boudraa, A., Gonnaud, P.M., Mallet, J.J., Sappey-Marinier, D., 2001. Regional differences and metabolic changes in normal aging of the human brain: proton MR spectroscopic imaging study. Am. J. Neuroradiol. 22, 119–127.

Apkarian, A.V., Sosa, Y., Sonty, S., Levy, R.M., Harden, R.N., Parrish, T.B., Gitelman, D.R., 2004. Chronic back pain is associated with decreased prefrontal and thalamic gray matter density. J. Neurosci. 24, 10410–10415.

Baliki, M.N., Petre, B., Torbey, S., Herrmann, K.M., Huang, L., Schnitzer, T.J., Fields, H.L., Apkarian, A.V., 2012. Corticostriatal functional connectivity predicts transition to chronic back pain. Nat. Neurosci. 15, 1117–1119.

Becerra, L., Morris, S., Bazes, S., Gostic, R., Sherman, S., Gostic, J., Pendse, G., Moulton, E., Scrivani, S., Keith, D., Chizh, B., Borsook, D., 2006. Trigeminal neuropathic pain alters responses in CNS circuits to mechanical (brush) and thermal (cold and heat) stimuli. J. Neurosci. 26, 10646–10657.

Bie, B., Brown, D.L., Naguib, M., 2011. Increased synaptic GluR1 subunits in the anterior cingulate cortex of rats with peripheral inflammation. Eur. J. Pharmacol. 653, 26–31.

Blom, S.M., Pfister, J.P., Santello, M., Senn, W., Nevian, T., 2014. Nerve injury-induced neuropathic pain causes disinhibition of the anterior cingulate cortex. J. Neurosci. 34, 5754–5764.

Bluml, S., Wisnowski, J.L., Nelson Jr., M.D., Paquette, L., Gilles, F.H., Kinney, H.C., Panigrahy, A., 2013. Metabolic maturation of the human brain from birth through adolescence: insights from in vivo magnetic resonance spectroscopy. Cereb. Cortex 23, 2944–2955.

Bolliger, C.S., Boesch, C., Kreis, R., 2013. On the use of Cramer–Rao minimum variance bounds for the design of magnetic resonance spectroscopy experiments. NeuroImage 83, 1031–1040.

Borsook, D., Becerra, L., 2011. CNS animal fMRI in pain and analgesia. Neurosci. Biobehav. Rev. 35, 1125–1143.

Cao, X.Y., Xu, H., Wu, L.J., Li, X.Y., Chen, T., Zhuo, M., 2009. Characterization of intrinsic properties of cingulate pyramidal neurons in adult mice after nerve injury. Mol. Pain 5, 73.

Chang, P.C., Pollema-Mays, S.L., Centeno, M.V., Procissi, D., Contini, M., Baria, A.T., Martina, M., Apkarian, A.V., 2014. Role of nucleus accumbens in neuropathic pain: linked multi-scale evidence in the rat transitioning to neuropathic pain. Pain 155, 1128–1139.

Chaplan, S.R., Bach, F.W., Pogrel, J.W., Chung, J.M., Yaksh, T.L., 1994. Quantitative assessment of tactile allodynia in the rat paw. J. Neurosci. Methods 53, 55–63.

Choi, Y., Yoon, Y.W., Na, H.S., Kim, S.H., Chung, J.M., 1994. Behavioral signs of ongoing pain and cold allodynia in a rat model of neuropathic pain. Pain 59, 369–376.

Craft, R.M., Mogil, J.S., Aloisi, A.M., 2004. Sex differences in pain and analgesia: the role of gonadal hormones. Eur. J. Pain 8, 397–411.

Davis, K.D., Taylor, K.S., Anastakis, D.J., 2011. Nerve injury triggers changes in the brain. Neuroscientist 17, 407–422.

Decosterd, I., Woolf, C.J., 2000. Spared nerve injury: an animal model of persistent peripheral neuropathic pain. Pain 87, 149–158.

D'Souza, D.V., Jonckers, E., Bruns, A., Künnecke, B., von Kienlin, M., Van der Linden, A., Mueggler, T., Verhoye, M., 2014. Preserved modular network organization in the sedated rat brain. PLoS ONE 9, 1–10.

Erecinska, M., Silver, I.A., 1990. Metabolism and role of glutamate in mammalian brain. Prog. Neurobiol. 35, 245–296.

Fillingim, R.B., Ness, T.J., 2000. Sex-related hormonal influences on pain and analgesic responses. Neurosci. Biobehav. Rev. 24, 485–501.

Frye, C.A., Petralia, S.M., Rhodes, M.E., 2000. Estrous cycle and sex differences in performance on anxiety tasks coincide with increases in hippocampal progesterone and 3alpha,5alpha-THP. Pharmacol. Biochem. Behav. 67, 587–596.

Gong, K.R., Cao, F.L., He, Y., Gao, C.Y., Wang, D.D., Li, H., Zhang, F.K., An, Y.Y., Lin, Q., Chen, J., 2010. Enhanced excitatory and reduced inhibitory synaptic transmission contribute to persistent pain-induced neuronal hyper-responsiveness in anterior cingulate cortex. Neuroscience 171, 1314–1325.

Hashmi, J.A., Baliki, M.N., Huang, L., Baria, A.T., Torbey, S., Hermann, K.M., Schnitzer, T.J., Apkarian, A.V., 2013. Shape shifting pain: chronification of back pain shifts brain representation from nociceptive to emotional circuits. Brain 136, 2751–2768.

Johnston, A.L., File, S.E., 1991. Sex differences in animal tests of anxiety. Physiol. Behav. 49, 245–250.

Khan, S.A., Keaser, M.L., Meiller, T.F., Seminowicz, D.A., 2014. Altered structure and function in the hippocampus and medial prefrontal cortex in patients with burning mouth syndrome. Pain 155, 1472–1480.

Kokras, N., Dalla, C., 2014. Sex differences in animal models of psychiatric disorders. Br. J. Pharmacol. 171, 4595–4619.

Kontinen, V.K., Kauppila, T., Paananen, S., Pertovaara, A., Kalso, E., 1999. Behavioural measures of depression and anxiety in rats with spinal nerve ligation-induced neuropathy. Pain 80, 341–346.

Leite-Almeida, H., Meida-Torres, L., Mesquita, A.R., Pertovaara, A., Sousa, N., Cerqueira, J.J., Almeida, A., 2009. The impact of age on emotional and cognitive behaviours triggered by experimental neuropathy in rats. Pain 144, 57–65.

Leith, J.L., Koutsikou, S., Lumb, B.M., Apps, R., 2010. Spinal processing of noxious and innocuous cold information: differential modulation by the periaqueductal gray. J. Neurosci. 30, 4933–4942.

Li, W., Wang, P., Li, H., 2014. Upregulation of glutamatergic transmission in anterior cingulate cortex in the diabetic rats with neuropathic pain. Neurosci. Lett. 568, 29–34.

Liu, Z.M., Schmidt, K.F., Sicard, K.M., Duong, T.Q., 2004. Imaging oxygen consumption in forepaw somatosensory stimulation in rats under isoflurane anesthesia. Magn. Reson. Med. 52, 277–285.

Liu, X., Zhu, X., Zhang, Y., Chen, W., 2013. The change of functional connectivity specificity in rats under various anesthesia levels and its neural origin. Brain Topogr. 26, 363–377.

Low, L.A., Millecamps, M., Seminowicz, D.A., Naso, L., Thompson, S.J., Stone, L.S., Bushnell, M.C., 2012. Nerve injury causes long-term attentional deficits in rats. Neurosci. Lett. 529, 103–107.

Maihofner, C., Handwerker, H.O., Birklein, F., 2006. Functional imaging of allodynia in complex regional pain syndrome. Neurology 66, 711–717.

Mantyh, P.W., 1982. Forebrain projections to the periaqueductal gray in the monkey, with observations in the cat and rat. J. Comp. Neurol. 206, 146–158.

Marchand, J.E., Hagino, N., 1983. Afferents to the periaqueductal gray in the rat. A horseradish peroxidase study. Neuroscience 9, 95–106.

Please cite this article as: Hubbard, C.S., et al., Behavioral, metabolic and functional brain changes in a rat model of chronic neuropathic pain: A longitudinal MRI study, NeuroImage (2014), http://dx.doi.org/10.1016/j.neuroimage.2014.12.024

Masamoto, K., Kim, T., Fukuda, M., Wang, P., Kim, S., 2007. Relationship between neural, vascular, and BOLD signals in isoflurane-anesthetized rat somatosensory cortex. Cereb. Cortex 17, 942–950.
May, A., 2008. Chronic pain may change the structure of the brain. Pain 137, 7–15.
Mayer, D.J., Liebeskind, J.C., 1974. Pain reduction by focal electrical stimulation of the brain: an anatomical and behavioral analysis. Brain Res. 68, 73–93.
Mika, J., Zychowska, M., Popiolek-Barczyk, K., Rojewska, E., Przewlocka, B., 2013. Importance of glial activation in neuropathic pain. Eur. J. Pharmacol. 716, 106–119.
Mogil, J.S., 2012. Sex differences in pain and pain inhibition: multiple explanations of a controversial phenomenon. Nat. Rev. Neurosci. 13, 859–866.
Mogil, J.S., Chanda, M.L., 2005. The case for the inclusion of female subjects in basic science studies of pain. Pain 117, 1–5.
Mullins, P.G., Rowland, L.M., Jung, R.E., Sibbitt, W.L., 2005. A novel technique to study the brain's response to pain: proton magnetic resonance spectroscopy. NeuroImage 26, 642–646.
Mutso, A.A., Radzicki, D., Baliki, M.N., Huang, L., Banisadr, G., Centeno, M.V., Radulovic, J., Martina, M., Miller, R.J., Apkarian, A.V., 2012. Abnormalities in hippocampal functioning with persistent pain. J. Neurosci. 32, 5747–5756.
Paban, V., Fauvelle, F., Alescio-Lautier, B., 2010. Age-related changes in metabolic profiles of rat hippocampus and cortices. Eur. J. Neurosci. 31, 1063–1073.
Paller, C.J., Campbell, C.M., Edwards, R.R., Dobs, A.S., 2009. Sex-based differences in pain perception and treatment. Pain Med. 10, 289–299.
Paxinos, G., Watson, R., 2005. The Rat Brain in Stereotaxic Coordinates. Elsevier Academic Press, New York.
Peyron, R., Schneider, F., Faillenot, I., Convers, P., Barral, F.G., Garcia-Larrea, L., Laurent, B., 2004. An fMRI study of cortical representation of mechanical allodynia in patients with neuropathic pain. Neurology 63, 1838–1846.
Pritchard, L.M., Van Kempen, T.A., Zimmerberg, B., 2013. Behavioral effects of repeated handling differ in rats reared in social isolation and environmental enrichment. Neurosci. Lett. 536, 47–51.
Provencher, S.W., 2001. Automatic quantitation of localized in vivo 1H spectra with LCModel. NMR Biomed. 14, 260–264.
Reynolds, D.V., 1969. Surgery in the rat during electrical analgesia induced by focal brain stimulation. Science 164, 444–445.
Rodgers, R.J., Cole, J.C., 1993. Influence of social isolation, gender, strain, and prior novelty on plus-maze behaviour in mice. Physiol. Behav. 54, 729–736.
Ross, B.D., Bluml, S., Cowan, R., Danielsen, E., Farrow, N., Tan, J., 1998. In vivo MR spectroscopy of human dementia. Neuroimaging Clin. N. Am. 8, 809–822.
Sakata, S., Shima, F., Kato, M., Fukui, M., 1988. Effects of thalamic parafascicular stimulation on the periaqueductal gray and adjacent reticular formation neurons. A possible contribution to pain control mechanisms. Brain Res. 451, 85–96.
Sandkuhler, J., 2009. Models and mechanisms of hyperalgesia and allodynia. Physiol. Rev. 89, 707–758.
Schmitt, U., Hiemke, C., 1998. Combination of open field and elevated plus-maze: a suitable test battery to assess strain as well as treatment differences in rat behavior. Prog. Neuro-Psychopharmacol. Biol. Psychiatry 22, 1197–1215.
Seminowicz, D.A., Laferriere, A.L., Millecamps, M., Yu, J.S.C., Coderre, T.J., Bushnell, M.C., 2009. MRI structural brain changes associated with sensory and emotional function in a rat model of long-term neuropathic pain. NeuroImage 47, 1007–1014.
Seminowicz, D.A., Jiang, L., Ji, Y., Xu, S., Gullapalli, R.P., Masri, R., 2012. Thalamocortical asynchrony in conditions of spinal cord injury pain in rats. J. Neurosci. 32, 15843–15848.
Sorge, R.E., Martin, L.J., Isbester, K.A., Sotocinal, S.G., Rosen, S., Tuttle, A.H., Wieskopf, J.S., Acland, E.L., Dokova, A., Kadoura, B., Leger, P., Mapplebeck, J.C., McPhail, M., Delaney, A., Wigerblad, G., Schumann, A.P., Quinn, T., Frasnelli, J., Svensson, C.I., Sternberg, W.F., Mogil, J.S., 2014. Olfactory exposure to males, including men, causes stress and related analgesia in rodents. Nat. Methods 11, 629–632.
Stamford, J.A., 1995. Descending control of pain. Br. J. Anaesth. 75, 217–227.
Tang, J.S., Qu, C.L., Huo, F.Q., 2009. The thalamic nucleus submedius and ventrolateral orbital cortex are involved in nociceptive modulation: a novel pain modulation pathway. Prog. Neurobiol. 89, 383–389.
Thompson, S.J., Bushnell, M.C., 2012. Rodent functional and anatomical imaging of pain. Neurosci. Lett. 520, 131–139.
Vertes, R.P., 2006. Interactions among the medial prefrontal cortex, hippocampus and midline thalamus in emotional and cognitive processing in the rat. Neuroscience 142, 1–20.
Vogt, B.A., Paxinos, G., 2014. Cytoarchitecture of mouse and rat cingulate cortex with human homologies. Brain Struct. Funct. 219, 185–192.
Vogt, B.A., Sikes, R.W., 2000. The medial pain system, cingulate cortex, and parallel processing of nociceptive information. Prog. Brain Res. 122, 223–235.
Vogt, B.A., Finch, D.M., Olson, C.R., 1992. Functional heterogeneity in cingulate cortex: the anterior executive and posterior evaluative regions. Cereb. Cortex 2, 435–443.
Walsh, R.N., Cummins, R.A., 1976. The Open-Field Test: a critical review. Psychol. Bull. 83, 482–504.
Witting, N., Kupers, R.C., Svensson, P., Jensen, T.S., 2006. A PET activation study of brush-evoked allodynia in patients with nerve injury pain. Pain 120, 145–154.
Wu, L.J., Toyoda, H., Zhao, M.G., Lee, Y.S., Tang, J., Ko, S.W., Jia, Y.H., Shum, F.W., Zerbinatti, C.V., Bu, G., Wei, F., Xu, T.L., Muglia, L.J., Chen, Z.F., Auberson, Y.P., Kaang, B.K., Zhuo, M., 2005. Upregulation of forebrain NMDA NR2B receptors contributes to behavioral sensitization after inflammation. J. Neurosci. 25, 11107–11116.
Xu, H., Wu, L.J., Wang, H., Zhang, X., Vadakkan, K.I., Kim, S.S., Steenland, H.W., Zhuo, M., 2008. Presynaptic and postsynaptic amplifications of neuropathic pain in the anterior cingulate cortex. J. Neurosci. 28, 7445–7453.
Xu, S., Ji, Y., Chen, X., Yang, Y., Gullapalli, R.P., Masri, R., 2013. In vivo high-resolution localized (1) H MR spectroscopy in the awake rat brain at 7 T. Magn. Reson. Med. 69, 937–943.
Yaksh, T.L., Al-Rodhan, N.R., Jensen, T.S., 1988. Sites of action of opiates in production of analgesia. Prog. Brain Res. 77, 371–394.
Zhang, X., Liu, H., Wu, J., Zhang, X., Liu, M., Wang, Y., 2009. Metabonomic alterations in hippocampus, temporal and prefrontal cortex with age in rats. Neurochem. Int. 54, 481–487.
Zhao, M.G., Ko, S.W., Wu, L.J., Toyoda, H., Xu, H., Quan, J., Li, J., Jia, Y., Ren, M., Xu, Z.C., Zhuo, M., 2006. Enhanced presynaptic neurotransmitter release in the anterior cingulate cortex of mice with chronic pain. J. Neurosci. 26, 8923–8930.
Zhuo, M., Wu, G., Wu, L.J., 2011. Neuronal and microglial mechanisms of neuropathic pain. Mol. Brain 4, 31–43.
Zimmerberg, B., Farley, M.J., 1993. Sex differences in anxiety behavior in rats: role of gonadal hormones. Physiol. Behav. 54, 1119–1124.

Please cite this article as: Hubbard, C.S., et al., Behavioral, metabolic and functional brain changes in a rat model of chronic neuropathic pain: A longitudinal MRI study, NeuroImage (2014), http://dx.doi.org/10.1016/j.neuroimage.2014.12.024